Langmuir
Article

pubs.acs.org/Langmuir

Importance of Trimethylaluminum Diffusion in Three-Step ABC Molecular Layer Deposition Using Trimethylaluminum, Ethanolamine, and Maleic Anhydride

Dragos Seghete,[†] Robert A. Hall,[†,‡] Byunghoon Yoon,[†] and Steven M. George*[,†,‡,§]

[†]*Department of Chemistry and Biochemistry,* [‡]*DARPA Center for Integrated Micro/Nano-Electromechanical Transducers (iMINT), and* [§]*Department of Chemical and Biological Engineering, University of Colorado at Boulder, Boulder, Colorado 80309, United States*

Received July 1, 2010. Revised Manuscript Received September 25, 2010

Hybrid organic−inorganic films were grown by molecular layer deposition (MLD) with a three-step ABC reaction sequence using (A) trimethylaluminum (TMA), (B) ethanolamine (EA), and (C) maleic anhydride (MA) at 90 °C. Very large steady state mass gains of 1854−4220 ng/(cm^2 cycle) were measured depending on reaction conditions. These mass gains are much larger than typical mass gains for surface reactions. The quartz crystal microbalance (QCM) mass profiles during the TMA reaction were consistent with TMA diffusion into and out of the ABC films. The ABC mass gains per cycle also displayed a strong dependence on the TMA dose and purge times that was consistent with the effects of TMA diffusion. Multiple dose experiments conducted at 130 °C revealed that the ABC reactions were self-limiting for thin ABC films. For thicker ABC films, increased TMA diffusion into the ABC film led to non-self-limiting behavior. Numerical modeling assuming Fickian diffusion for TMA diffusing into and out of the ABC film could fit the QCM mass profiles. The results all indicate that TMA diffusion into the ABC MLD film plays a key role in the thin film growth. In addition, X-ray reflectivity (XRR) measurements revealed that the ABC films were exceptionally smooth.

I. Introduction

Atomic layer deposition (ALD) is a thin film synthesis method for inorganic materials based on sequential, self-limiting surface reactions.[1−3] Because of its accurate control of thickness and high conformality, ALD is useful in nanofabrication and nanostructure engineering.[4] Molecular layer deposition (MLD) is an extension of ALD to include films that contain organic molecular components.[5,6] Entirely organic MLD systems that have been studied include polyamides,[7,8] polyimides,[6,9] and polyureas.[10,11] Other MLD systems have been investigated where an organic molecular precursor is combined with an inorganic ALD precursor to produce hybrid organic−inorganic MLD films.[5,12−17] One of the first hybrid systems was obtained by sequential exposures of trimethylaluminum (TMA) and ethylene glycol (EG)[12] to produce aluminum alkoxide films known as alucones.[18] A variety of hybrid MLD systems have been studied either by varying the organic molecular precursor[5,14,19] or changing the inorganic precursor.[13,15,16]

Most of the MLD systems to date have been based on two-step AB binary reaction schemes that have employed homobifunctional reactants.[5,7,12,20] The EG precursor in the TMA + EG alucone reaction is an example of a homobifunctional precursor because EG has two hydroxyl groups on an ethylene backbone.[12] One consequence of homobifunctional precursors is the possibility of "double" reactions that can occur between the substrate and the homobifunctional precursor.[5,12] These double reactions can reduce the number of active surface sites and reduce the growth rate. Double reactions have been proposed as a growth inhibitor for alucone,[12] zincone,[15,16] and other all-organic MLD films.[7]

A novel three-step ABC system was recently explored to circumvent the double reaction problems.[17] This ABC system is based on a reaction scheme consisting of (A) TMA as a homotrifunctional inorganic precursor, (B) ethanolamine (EA) as a heterobifunctional organic reactant, and (C) maleic anhydride (MA) as a ring-opening organic reactant.[5,17] The initial study of the ABC MLD system employed *in situ* Fourier transform infrared (FTIR) spectroscopy to study the surface chemistry.[17] ABC MLD has also been employed as a sacrificial layer in the fabrication of nanoelectromechanical systems (NEMS).[21]

*To whom correspondence should be addressed.

(1) George, S. M. *Chem. Rev.* **2010**, *110*, 111.
(2) Puurunen, R. L. *J. Appl. Phys.* **2005**, *97*, 121301.
(3) Suntola, T. *Thin Solid Films* **1992**, *216*, 84.
(4) Knez, M.; Niesch, K.; Niinisto, L. *Adv. Mater.* **2007**, *19*, 3425.
(5) George, S. M.; Yoon, B.; Dameron, A. A. *Acc. Chem. Res.* **2009**, *42*, 498.
(6) Yoshimura, T.; Tatsuura, S.; Sotoyama, W. *Appl. Phys. Lett.* **1991**, *59*, 482.
(7) Adamczyk, N. M.; Dameron, A. A.; George, S. M. *Langmuir* **2008**, *24*, 2081.
(8) Shao, H.-I.; Umemoto, S.; Kikutani, T.; Okui, N. *Polymer* **1997**, *38*, 459.
(9) Putkonen, M.; Harjuoja, J.; Sajavaara, T.; Niinisto, L. *J. Mater. Chem.* **2007**, *17*, 664.
(10) Kim, A.; Filler, M. A.; Kim, S.; Bent, S. F. *J. Am. Chem. Soc.* **2005**, *127*, 6123.
(11) Loscutoff, P. W.; Zhou, H.; Clendenning, S. B.; Bent, S. F. *ACS Nano* **2009**, *4*, 331.
(12) Dameron, A. A.; Seghete, D.; Burton, B. B.; Davidson, S. D.; Cavanagh, A. S.; Bertrand, J. A.; George, S. M. *Chem. Mater.* **2008**, *20*, 3315.
(13) Lee, B. H.; Im, K. K.; Lee, K. H.; Im, S.; Sung, M. M. *Thin Solid Films* **2009**, *517*, 4056.
(14) Nilsen, O.; Klepper, K.; Nielsen, H.; Fjellvag, H. *ECS Trans.* **2008**, *16*, 3.
(15) Peng, Q.; Gong, B.; VanGundy, R. M.; Parsons, G. N. *Chem. Mater.* **2009**, *21*, 820.
(16) Yoon, B.; O'Patchen, J. L.; Seghete, D.; Cavanagh, A. S.; George, S. M. *Chem. Vap. Deposition* **2009**, *15*, 112.
(17) Yoon, B.; Seghete, D.; Cavanagh, A. S.; George, S. M. *Chem. Mater.* **2009**, *21*, 5365.
(18) McMahon, C. N.; Alemany, L.; Callender, R. L.; Bott, S. G.; Barron, A. R. *Chem. Mater.* **1999**, *11*, 3181.
(19) Nilsen, O.; Fjellvag, H. Patent Cooperation Treaty (PCT), World Intellectual Property Organization, Publication Number WO 2006/071126 A1, Publication Date July 6, 2006. Title: "Thin Films Prepared with Gas Phase Deposition Technique".
(20) George, S. M.; Ott, A. W.; Klaus, J. W. *J. Phys. Chem.* **1996**, *100*, 13121.
(21) Seghete, D.; Davidson, B. D.; Hall, R. A.; Chang, Y. J.; Bright, V. M.; George, S. M. *Sens. Actuators, A* **2009**, *155*, 8.

Report Documentation Page

Form Approved
OMB No. 0704-0188

1. REPORT DATE	2. REPORT TYPE	3. DATES COVERED
SEP 2010		**00-00-2010 to 00-00-2010**

4. TITLE AND SUBTITLE	5a. CONTRACT NUMBER
Importance of Trimethylaluminum Diffusion in Three-Step ABC Molecular Layer Deposition Using Trimethylaluminum, Ethanolamine, and Maleic Anhydride	5b. GRANT NUMBER
	5c. PROGRAM ELEMENT NUMBER
6. AUTHOR(S)	5d. PROJECT NUMBER
	5e. TASK NUMBER
	5f. WORK UNIT NUMBER
7. PERFORMING ORGANIZATION NAME(S) AND ADDRESS(ES) **University of Colorado,Department of Chemistry and Biochemistry,Boulder,CO,80309**	8. PERFORMING ORGANIZATION REPORT NUMBER
9. SPONSORING/MONITORING AGENCY NAME(S) AND ADDRESS(ES)	10. SPONSOR/MONITOR'S ACRONYM(S)
	11. SPONSOR/MONITOR'S REPORT NUMBER(S)

12. DISTRIBUTION/AVAILABILITY STATEMENT
Approved for public release; distribution unlimited

13. SUPPLEMENTARY NOTES

14. ABSTRACT

15. SUBJECT TERMS

16. SECURITY CLASSIFICATION OF:			17. LIMITATION OF ABSTRACT	18. NUMBER OF PAGES	19a. NAME OF RESPONSIBLE PERSON
a. REPORT **unclassified**	b. ABSTRACT **unclassified**	c. THIS PAGE **unclassified**	**Same as Report (SAR)**	**7**	

The surface reactions during ABC growth were proposed by the initial FTIR study:[17]

$$\text{(A)}\quad \mathrm{S-COOH^* + Al(CH_3)_3} \rightarrow \mathrm{S-COO-Al(CH_3)_2^* + CH_4} \qquad (1)$$

$$\text{(B)}\quad \mathrm{S-AlCH_3^* + HO(CH_2)_2NH_2} \rightarrow \mathrm{S-Al-O(CH_2)_2NH_2^* + CH_4} \qquad (2)$$

$$\text{(C)}\quad \mathrm{S-NH_2^* + C_4H_2O_3(MA)} \rightarrow \mathrm{S-NH-C(O)CHCH-COOH^*} \qquad (3)$$

In these reactions, the asterisks designate the reactive surface species and S denotes the substrate including the reaction products from the previous reactions. TMA reacts with the hydroxyls of the surface carboxylic acid groups to produce $AlCH_3$* surface functionalities as shown in eq 1. The $AlCH_3$* species react with the hydroxyl moiety of EA to form $AlOCH_2CH_2NH_2$* upon EA exposure, as given in eq 2. MA then reacts with the amine surface functionality in a ring-opening reaction to regenerate the carboxylic acid groups on the surface, as illustrated in eq 3.

In this paper, the ABC MLD system is investigated using *in situ* QCM studies in a viscous flow reactor. The nucleation and growth of ABC MLD were examined on the Al_2O_3 ALD surface. The time-dependent QCM studies are ideal to monitor the mass gains and losses during the individual TMA, EA, and MA reactions. The QCM measurements can monitor the nucleation of ABC growth prior to the development of an ABC film. In addition, the QCM can observe the diffusion of TMA into and out of the ABC film. The ABC growth was examined versus TMA exposure time and purge time after the TMA exposure. These studies corroborate the importance of TMA diffusion during ABC film growth.

II. Experimental Section

A. Viscous Flow Reactor and Precursors. All ABC films were fabricated in a viscous flow reactor that has been described in detail elsewhere.[22] A constant flow of N_2 carrier gas at a total rate of 160 sccm passed through the reactor. This N_2 gas flow yielded a base pressure of ~0.8 Torr. The temperature of the reactor was maintained using an external ceramic heater. Pressure was measured using a bakeable capacitance manometer (MKS, Model 121). The precursors were introduced into the reactor by opening pneumatic valves.

Trimethylaluminum (97%) and maleic anhydride (98%) were obtained from Sigma-Aldrich (St. Louis, MO). Ethanolamine (98%) was obtained from Gelest (Philadelphia, PA). All chemicals were used as received. The transfer of EA and MA into stainless steel dosing vessels occurred in a dry N_2-filled glovebag. To extract any potential H_2O impurities, 2 g of activated 4 Å molecular sieves from Mallinckrodt (Philipsburg, NJ) was added to the EA precursor vessel.

Two schemes were used for the deposition of the ABC films. The first scheme involved consecutive doses of each precursor in the order TMA, EA, MA, separated by purges. The pulse sequence was defined by (t_1, t_2, t_3, t_4, t_5, t_6), where t_1 is the TMA exposure time, t_2 is the purge time after the TMA exposure, t_3 is the EA exposure time, t_4 is the purge time after the EA exposure, t_5 is the MA exposure time, and t_6 is the purge time after the MA exposure. In the second scheme, each precursor was dosed multiple times consecutively. In this multiple dose scheme, the pulse sequence is designated as $a(t_i,t_j)$, where a is the number of consecutive doses, t_i is the exposure time, and t_j is the purge time.

Dosing systems for high vapor pressure precursors are based on the diffusion of the precursor either directly into the ALD reactor or directly into a N_2 gas stream that entrains and transports the precursor into the ALD reactor. These dosing setups have been described previously and have been utilized for TMA dosing.[22,23] When the pressure inside the precursor vessel is lower than the operating pressure of the reactor, very little precursor can diffuse into the reactor. To circumvent this dosing problem, the N_2 carrier gas was diverted through the headspace of the precursor vessel. This dosing design was used for EA and MA.

B. Quartz Crystal Microbalance Analysis. A detailed description of the *in situ* QCM experimental setup has been given elsewhere.[22,23] The QCM sensors were AT-cut quartz crystals with a polished Au face and a 6 MHz oscillation frequency. These QCM sensors were obtained from Colorado Crystal Corp (Loveland, CO). The crystals were fitted onto a modified Maxtek BSH-150 sensor head connected to a Maxtek TM-400 monitor obtained from Inficon (East Syracuse, NY). The QCM housing was purged with N_2 that introduced an additional 100 mTorr of N_2 in the reactor. Prior to the MLD experiments, the Au-coated QCM crystal was covered with a ~200 Å thick Al_2O_3 ALD film to ensure reproducibility. Between the MLD experiments, Al_2O_3 ALD was also grown to regenerate a reproducible starting surface and to monitor the performance of the QCM crystal. The quartz crystal was replaced whenever the Al_2O_3 ALD growth rate deviated from ideal growth behavior.[23]

C. X-ray Reflectivity. *Ex situ* X-ray reflectivity (XRR) measurements were recorded on a Bede D1 diffractometer from Jordan Valley Semiconductor (Austin, TX). The diffractometer was equipped with a Cu Kα X-ray tube with a wavelength of 1.54 Å and a Max-flux focusing optics from Rigaku, Inc. (The Woodlands, TX). The incident beam was further conditioned by a channel-cut crystal and 0.5 mm wide source and detector slits. A filament current of 40 mA and a voltage of 40 kV were used for all experiments. All XRR scans were performed with an 8 arcsec step size and a 5 s acquisition time. Obtained data were fit to extract film thickness, density, and surface roughness using the Bede REFS software.

For *ex situ* XRR analysis, the MLD films were grown onto 1 in. by 1 in. square samples cleaved from boron-doped p-type Si(100) wafers with a thin native oxide. These Si(100) wafers were obtained from Silicon Valley Semiconductors, Inc. (Santa Clara, CA). Prior to deposition, each sample was rinsed with water, acetone, and isopropyl alcohol and then dried in an ultrahigh-purity N_2 stream.

D. Modeling of TMA Diffusion. Numerical simulations of the diffusion of the TMA molecule into and out of the ABC film were performed using Mathematica, Version 7.0, from Wolfram Research Inc. (Champaign, IL). Fick's second law of diffusion was solved numerically using the "NDSolve" package and the "StiffnessSwitching" method. The concentration of TMA inside the ABC film at a distance x from the film surface at time t was denoted by the function $C(x,t)$. Assuming ideal diffusion behavior, $C(x,t)$ was calculated numerically from the following system of equations:

$$\frac{\partial C}{\partial t} = D\frac{\partial^2 C}{\partial x^2} \qquad (4)$$

$$\frac{\partial C}{\partial x} = 0, \quad x = x_{\max} \qquad (5)$$

$$C(x,0) = C_0 \qquad (6)$$

$$C(0,t) = C_s \qquad (7)$$

where D is the diffusion coefficient for TMA and $x_{\max}$ is the maximum diffusion distance, i.e., the ABC film thickness. C_0 is the initial TMA concentration in the ABC film at $t = 0$, and C_s is the concentration of TMA at the surface of the ABC film. The

(22) Elam, J. W.; Groner, M. D.; George, S. M. *Rev. Sci. Instrum.* **2002**, *73*, 2981.

(23) Wind, R. A.; George, S. M. *J. Phys. Chem. A* **2010**, *114*, 1281.

magnitudes of the variables were selected to match the experimental conditions: a TMA dose time of 200 s, a TMA purge time of 800 s, and an estimated ABC film thickness of 400 Å. Equation 4 is the one-dimensional form of Fick's second law of diffusion with a constant diffusion coefficient. Equation 5 ensures that $C(x,t)$ is a continuous function at the bottom boundary of the ABC film. Equations 6 and 7 are boundary conditions in time and space, respectively.

Initially at $t = 0$, there is no TMA in the ABC film and $C_0 = 0$ in eq 6. During the TMA exposure, the concentration of TMA on the surface of the ABC film was assumed to be constant at $C_s = 0.81$ g/cm^3 in eq 7. This value of C_s is the density of liquid TMA. Using the density of liquid TMA presupposes that the TMA is present as a multilayer on the surface during the TMA exposures. The concentration profile at the end of the 200 s diffusion process, $C(x,200)$, was used as the starting point for the calculation of TMA diffusion out of the film. C_s was assumed to be $C_s = 0$ during TMA diffusion out of the ABC film. The TMA concentration profile, $C(x,t)$, was translated into the total TMA mass in the ABC film, $M(t)$, using

$$M(t) = \int_0^{x_{max}} C(x,t)\,dx \qquad (8)$$

where $M(t)$ has units of ng/cm^2.

III. Results and Discussion

A. Mass Gain during ABC Growth and Evidence for TMA Diffusion. Figure 1 shows a typical QCM mass gain obtained during the first 45 cycles of ABC MLD on an Al_2O_3 ALD surface at 90 °C using a pulse sequence of (6, 90, 6, 60, 6, 60). Similar QCM results were also obtained at higher temperatures. The large dosing and purging timings were chosen to ensure complete reactions and removal of reactants and products. The deposition of the ABC film can be described by three different growth regions. A nearly constant mass gain of 70 ng/(cm^2 cycle) is observed in region I during the first 10 cycles. A rapid increase of the mass gain occurs in region II in the transition regime from cycles 11 to 28. The mass gain stabilizes at an average value of 3980 ng/(cm^2 cycle) in region III in the steady state regime from cycles 29 to 45.

The average mass gain of 3980 ng/(cm^2 cycle) in the linear region is very large compared with previous MLD systems. For example, the average mass gain for the TMA + EG alucone system grown at 85 °C was 58 ng/(cm^2 cycle).[12] The average mass gain for the diethylzinc (DEZ) + EG zincone system was 20.4 ng/(cm^2 cycle) at 135 °C.[16] The average mass gain for the well-known Al_2O_3 ALD system using TMA + H_2O is 35 ng/(cm^2 cycle) at 120 °C.[23] The large mass gain with excellent linear growth in region III is extraordinary and indicates that the ABC MLD growth cannot be described only by surface chemical reactions.

Figure 2 shows the QCM mass gains for two ABC cycles during region III in the steady state regime. A 300 s purge time was used for the data presented in Figure 2. The longer purge time with a pulse sequence of (6, 300, 6, 300, 6, 300) ensured more efficient reactant and product removal. Figure 2 shows that the TMA dose produced a large transient mass gain of ~2500 ng/cm^2. This large mass gain is followed by a subsequent rapid mass loss at the start of the purge period. The mass loss decreased after 100 s of purge time. A net mass gain of $\Delta m_A = 835$ ng/cm^2 was observed at the end of the TMA reaction and purge period.

A qualitatively similar behavior was observed when TMA was dosed onto various polymer-coated QCM crystals.[24] The large mass gain followed by a partial mass loss was attributed to TMA diffusion into and out of the polymer films.[24] Previous studies have also revealed the infiltration of metalorganic ALD precursors into various polymers such PMMA,[25] polypropylene,[26] and P3HT.[27] Given these earlier studies, the large mass gain and subsequent mass loss during the TMA dose and purge can be explained by the diffusion of the TMA precursor into and out of the ABC film.

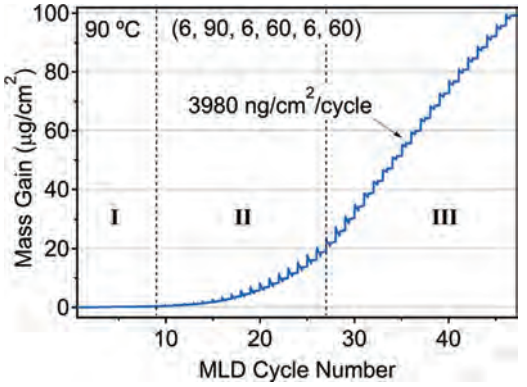

Figure 1. QCM mass gain during the first 45 cycles of ABC MLD film growth on an Al_2O_3 surface at 90 °C using TMA, EA, and MA with a pulse sequence of (6, 90, 6, 60, 6, 60).

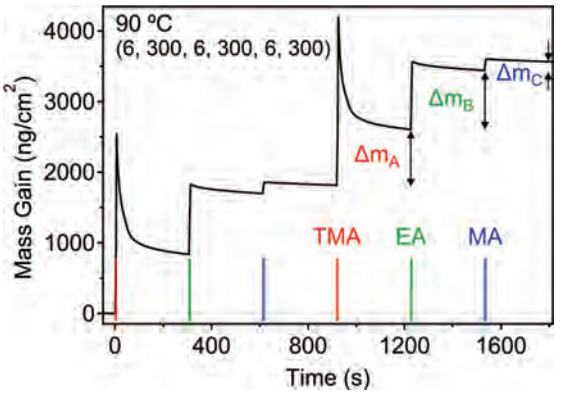

Figure 2. QCM mass gain for two cycles of ABC film growth in the linear growth region at 90 °C with a pulse sequence of (6, 300, 6, 300, 6, 300).

Another possible reason for the large mass transient during the TMA exposure could be the formation of a TMA multilayer on top of the ABC film. However, the mass of one TMA monolayer is ~40 ng/cm^2.[24] Consequently, the net mass gain of $\Delta m_A = 835$ ng/cm^2 observed in Figure 2 is equivalent to a TMA multilayer with a thickness of 21 monolayers. Previous surface science studies have shown that the formation of a stable TMA multilayer after TMA exposures is not possible at room temperature.[28] The formation of a stable TMA multilayer after TMA exposures is also not expected at 90 °C.

The process of diffusion of TMA into the ABC film can help to explain the three regions of ABC growth in Figure 1. A minimum thickness of ABC polymer is needed before TMA diffusion can

(24) Wilson, C. A.; Grubbs, R. K.; George, S. M. *Chem. Mater.* **2005**, *17*, 5625.

(25) Sinha, A.; Hess, D. W.; Henderson, C. L. *J. Vac. Sci. Technol. B* **2007**, *25*, 1721.

(26) Jur, J. S.; Spagnola, J. C.; Lee, K.; Gong, B.; Peng, Q.; Parsons, G. N. *Langmuir* **2010**, *26*, 8239.

(27) Ferrari, S.; Perissinotti, F.; Peron, E.; Fumagalli, L.; Natali, D.; Sampietro, M. *Org. Electron.* **2007**, *8*, 407.

(28) Sano, H.; Sakai, J.; Mizutani, G.; Ushioda, S. *J. Electron Spectrosc. Relat. Phenom.* **1993**, *64–65*, 865.

occur. The formation of this threshold ABC film is believed to correspond to region I. As the ABC film grows thicker, a larger volume of film is available for TMA diffusion. The growth of the ABC film with an increasing component from TMA diffusion leads to an increase in mass gain per cycle in region II. When the ABC film thickness is larger than the TMA diffusion distance, the growth rate reaches a constant steady state value as observed in region III.

B. Mass Gains during EA and MA Reactions. A mass gain of 987 ng/cm^2 is obtained after 6 s of EA exposure as shown in Figure 2. A slight mass loss then occurs during the purge period. There is a net mass gain of Δm_B = 863 ng/cm^2 at the end of the purge period. Assuming an EA surface reaction as given by eq 2, each $AlCH_3$* surface species reacts with an EA molecule to produce a net mass gain of 45 amu/site. Using a surface $AlCH_3$* density of ~6 nm^{-2} obtained from previous detailed QCM studies of the Al_2O_3 ALD growth,[23] the EA reaction in eq 2 would produce a mass gain of ~43 ng/(cm^2 cycle). The experimental net mass gain of 863 ng/cm^2 after the EA reaction is about 20 times greater than the estimated mass gain of ~43 ng/(cm^2 cycle) for the EA surface reaction given in eq 2. Therefore, the mass gains during the EA reaction cannot be explained by surface chemical reactions.

The discrepancy between the expected and measured mass gains suggests that EA reacts both with $AlCH_3$* surface species and TMA molecules in the ABC film. The existing ABC film acts as a TMA reservoir during the TMA exposures. Multiple monolayer equivalents of TMA remaining in the ABC film are believed to react with incoming gas phase EA molecules. The TMA + EA reaction is viewed as a chemical vapor deposition (CVD) reaction. If only the hydroxyl groups react, the result of the EA exposure would be the deposition of $Al(OCH_2CH_2NH_2)(CH_3)_2$, $Al(OCH_2CH_2NH_2)_2(CH_3)$, or $Al(OCH_2CH_2NH_2)_3$ monomers. These monomers are believed to remain in the ABC film and serve as seeds for the growth of new polymer chains.

The CVD reaction most likely occurs close to the surface of the ABC film because additional QCM experiments observed that EA does not diffuse into the ABC film. However, other QCM experiments demonstrated that the TMA + EA MLD reaction leads to continuous growth on a thick ABC film. In contrast, no MLD growth was observed for the TMA + EA MLD reaction on Al_2O_3 ALD surfaces. The TMA + EA reaction may also produce a cross-linked polymer if the $-NH_2$ amino group can react with TMA. This reaction is unlikely because the TMA reaction with $-NH_2$ groups does not occur efficiently until temperatures of > 320 °C during AlN ALD.[29,30]

A mass gain of 157 ng/cm^2 is then observed after a 6 s MA exposure in Figure 2. After a slight mass loss during the purge period, the net mass gain is Δm_C = 115 ng/(cm^2 cycle). In comparison, the MA surface reaction in eq 3 should lead to a net gain of 98 amu/site for each NH_2* species. Using a NH_2* surface site density of ~6 nm^{-2} based on $AlCH_3$* surface species during Al_2O_3 ALD,[23] the mass gain for a surface monolayer of NH_2* species would be ~94 ng/cm^2. There is reasonable agreement between this expected mass gain and the experimental mass gain of Δm_C = 115 ng/(cm^2 cycle). This agreement argues that the MA reaction is largely a surface reaction. The MA reacts with the NH_2* surface functionality as confirmed by the previous FTIR study.[17] The MA reaction may only be a surface reaction because MA is a much larger molecule and is unable to diffuse into the ABC film. In addition, TMA is not a factor because EA has already reacted with the TMA in the ABC film.

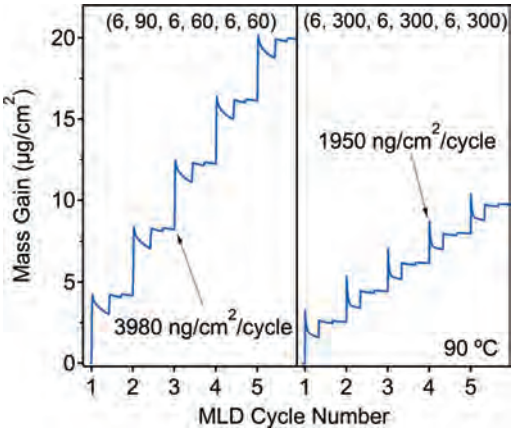

Figure 3. QCM mass gains for ABC film growth in the linear growth region at 90 °C for purge times of 90 s (left) and 300 s (right) with dosing times of 6 s for all the reactants.

C. Effect of Purge and Dose Times. The growth mechanism that emerges from Figure 2 suggests that TMA diffusion into and out of the MLD film plays a significant role in determining the growth rate of the ABC film. Additional experiments were performed to explore the effect of purge and dose times. Figure 3 shows the QCM mass gains for 5 MLD cycles during the linear growth regime for two ABC films grown at 90 °C with the same dose timings but different purge conditions. A large increase in purge time has the effect of reducing the average ABC growth rate. The purge times of 90 and 60 s following TMA and EA/MA exposures, respectively, yield a growth rate of 3980 ng/(cm^2 cycle). The longer purge time of 300 s following the TMA, EA, and MA exposures lowers the growth rate to 1950 ng/(cm^2 cycle).

The bulk of the reduction in mass gain is observed during the TMA reaction. For the short purge conditions, presented on the left side of Figure 3, the average individual mass gains were 2842, 1020, and 118 ng/cm^2 after the TMA, EA, and MA doses, respectively. For the long purge conditions, shown on the right side of Figure 3, the average individual mass gains were 971, 866, and 113 ng/cm^2 after the TMA, EA, and MA doses, respectively. Observing the majority of the mass gain reduction during the TMA reaction agrees well with the proposed TMA diffusion mechanism. Longer purges allow more time for TMA to diffuse out of the ABC film and yield smaller ABC MLD growth rates.

QCM studies also explored the effect of the TMA dose time on the ABC growth rate. QCM mass gains were measured in the linear growth region for three ABC films grown at 90 °C using TMA dose times of 4, 6, and 8 s. The average mass gains per ABC cycle were 3070, 3670, and 4220 ng/(cm^2 cycle), respectively. These results illustrate that the growth rate of the ABC MLD film can be tuned by varying the TMA dose time. The increasing growth rate with increasing TMA dose time is consistent with more TMA diffusion into the ABC film. The larger quantities of TMA react with EA and the TMA reaction does not display self-limiting behavior.

D. Results for Multiple Dosing Scheme. The growth behavior of the ABC MLD system was further investigated using a multiple dosing scheme to determine the self-limiting behavior of the TMA, EA, and MA exposures. The multiple dosing scheme was (10(2, 90), 10(3, 30), 10(3, 30)). QCM mass gains were measured for 17 multidose MLD cycles performed at 130 °C. The higher temperature of 130 °C decreases TMA diffusion into the film, increases TMA diffusion out of the film, and delays the

(29) Mayer, T. M.; Rogers, J. W.; Michalske, T. A. *Chem. Mater.* **1991**, *3*, 641.
(30) Riihela, D.; Ritala, M.; Matero, R.; Leskela, M.; Jokinen, J.; Haussalo, P. *Chem. Vap. Deposition* **1996**, *2*, 277.

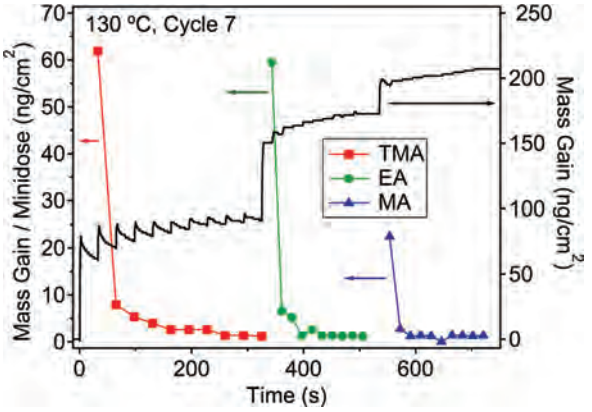

Figure 4. QCM mass gains and the mass gain per minidose for ABC film growth for the seventh multidose cycle in the transition region.

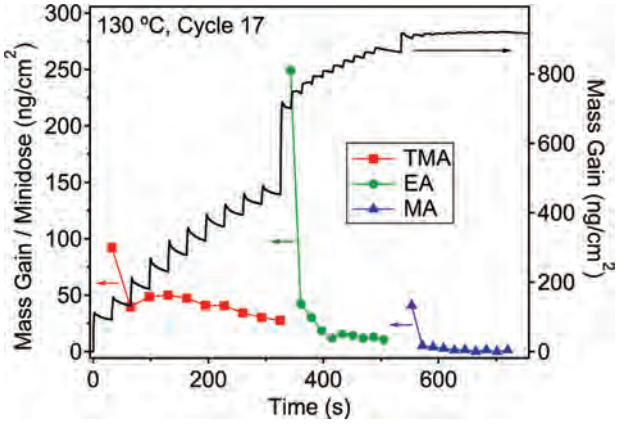

Figure 5. QCM mass gains and the mass gain per minidose for ABC film growth for the 17th multidose cycle in the linear growth region.

film nucleation. The growth reached the linear regime after ~10 MLD cycles at 130 °C. In comparison, the growth reached the linear regime after only ~3 MLD cycles for similar multidose experiments at 90 °C.

Results for individual MLD cycles during the multidose growth experiment provide insight into the self-limiting behavior and the effects of TMA diffusion. Figure 4 shows the QCM mass gains during the seventh MLD multidose cycle. Superimposed in Figure 4 are the mass gains per individual minidose. These mass gains are calculated as the QCM mass at the end of the purge period minus the QCM mass at the beginning of the dose period for each minidose. The seventh cycle is in the transition region at a total mass gain of 0.46 μg/cm^2 where the mass gain per cycle is increasing toward its large steady-state linear value. For the TMA minidoses, the largest mass gain of 62 ng/cm^2 was obtained during the first minidose. Further TMA minidoses led to consecutively decreasing mass gains per minidose as expected for a self-limiting reaction. A negligible mass gain was observed during the last 3 TMA minidoses. TMA diffusion does not lead to continued growth because there is very little ABC film available for TMA diffusion.

During the EA minidoses shown in Figure 4, the largest mass gain of 59 ng/cm^2 is obtained during the first EA minidose. The mass gains for the following EA minidoses decrease progressively and the last 5 minidoses add negligible mass as expected for a self-limiting reaction. The total mass gain for these EA minidoses was 81.5 ng/cm^2. A similar behavior was observed for the MA

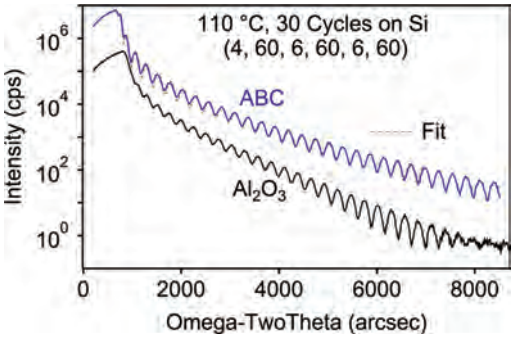

Figure 6. XRR scan for an ABC film with a thickness of 575 Å grown using 30 cycles on a silicon wafer at 110 °C with a pulse sequence of (4, 60, 6, 60, 6, 60). A second XRR scan for an Al_2O_3 ALD film with a comparable thickness of 573 Å is shown for comparison.

minidoses shown in Figure 4. The largest MA mass gain of 22 ng/cm^2 was obtained during the first minidose. There was a sharp decrease in mass gain for the following MA minidoses and a total mass gain per total MA dose of 33.5 ng/cm^2. The MA saturated the most rapidly of the three ABC precursors. The mass gains per MA minidose displayed self-limiting behavior and reached a negligible level after only 3 MA minidoses.

A different growth behavior is observed when focusing on the 17th multidose cycle during the linear growth region at a total mass gain of 7.70 μg/cm^2. Figure 5 shows the QCM mass gain and mass gains per minidose for the 17th MLD multidose cycle. The mass gains are much larger during the linear growth region during cycle 17 compared with the transition region in cycle 7. For the TMA minidoses, the first minidose is the largest with a mass gain of 92 ng/cm^2. The following 9 TMA minidoses also add considerable mass and do not display self-limiting behavior. These results are consistent with TMA continuing to diffuse into the ABC film. The total mass gain during the TMA minidoses was 453 ng/cm^2.

When compared with cycle 7, EA exposures during cycle 17 show a much larger mass gain of 249 ng/cm^2 during the first EA minidose in Figure 5. Subsequent EA minidoses are not self-limiting and the total mass gain for the EA minidoses was 410 ng/cm^2. The effect of the TMA diffusion into the ABC film has led to much higher mass gains during the EA minidoses. In comparison, the first MA minidose adds 40 ng/cm^2 in Figure 5, and the total mass gain was 55 ng/cm^2 for all the MA minidoses. The MA minidoses display self-limiting behavior and are similar to the MA minidoses in Figure 4 because the MA reaction is largely a surface reaction.

E. *Ex Situ* XRR Analysis. XRR was used for *ex situ* analysis of the ABC MLD films. Figure 6 shows the XRR scan of an ABC film after 30 cycles at 110 °C directly on a silicon wafer. The ABC film was modeled as a single homogeneous layer. The ABC film had a thickness of 575 Å, a density of 1.7 g/cm^3, and a root-mean-square roughness of 4.9 Å. The XRR scan of an Al_2O_3 ALD film with similar thickness to the ABC film of 573 Å is also displayed in Figure 6. The fitted roughness of this Al_2O_3 ALD film was 6.5 Å. The Al_2O_3 and ABC films had similar reflected intensity values. The XRR scan of the Al_2O_3 ALD film was displaced to lower intensity for clarity in presentation.

The measured roughness of the ABC film is remarkably low considering its large mass gain per cycle. The XRR scan of the Al_2O_3 ALD film in Figure 6 shows that the XRR oscillations lose amplitude and become noisy starting at 7000 arcsec. In contrast, the scan of the ABC sample maintains its oscillating amplitude beyond 8500 arcsec. The exceptional smoothness of the ABC film

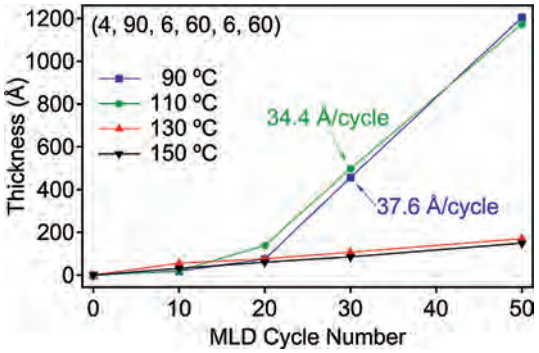

Figure 7. XRR measurements of the thickness of ABC films grown on silicon wafers versus number of MLD cycles for growth temperatures of 90, 110, 130, and 150 °C using a pulse sequence of (4, 90, 6, 60, 6, 60).

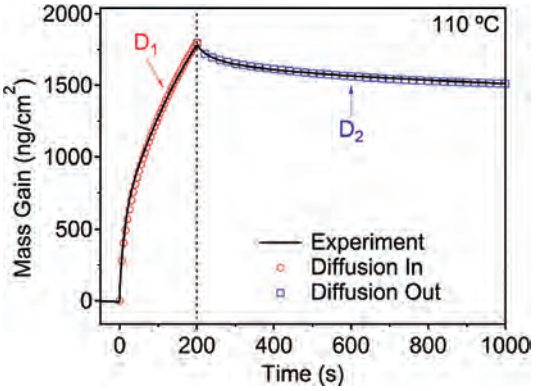

Figure 8. QCM mass gain during TMA dose for 200 s and then QCM mass loss for 800 s after the TMA dose. ABC film was grown using 30 cycles at 110 °C and had an estimated thickness of 400 Å. A fit to the mass gain and loss assuming TMA diffusion into and out of the film is shown for comparison.

can be attributed to the ABC film being in a glassy liquidlike state during growth. Previous studies have shown smoothing of polymer thin films with increasing temperature due to dynamic molecular rearrangement at the surface.[31] This process is known to take place in polymer thin films at temperatures below the glass transition temperature of bulk polymers.[31,32]

Figure 7 shows the thickness of ABC films measured by XRR versus the number of MLD cycles for various reaction temperatures. All ABC films were grown directly on silicon wafers using the same dosing conditions. The ABC films grown at 90 and 110 °C show an initial lower growth rate before reaching a linear growth region with growth rates of 34.4 and 37.6 Å/cycle, respectively. These XRR results are qualitatively similar to the QCM results in Figure 1. In contrast, the ABC growth at 130 and 150 °C remains low throughout the 50 MLD cycles in Figure 7. The residence times of TMA in the ABC film may be significantly reduced at these higher temperatures. Consequently, the CVD reaction between TMA and EA may be restricted without TMA in the ABC films.

The growth rate in the linear growth region was 37.6 Å/cycle at 90 °C. *In situ* QCM monitoring of the ABC MLD reaction at 90 °C using the same reaction conditions as shown in Figure 7 observed a mass gain of 1854 ng/(cm^2 cycle) in the linear growth region. The average density for the ABC films grown at 90 °C in the linear region was 1.7 g/cm^3 after exposure to air. Using the *ex situ* measured density, the *in situ* growth rate of the ABC film is calculated to be 109 Å/cycle. Therefore, there is a discrepancy between the *in situ* growth of 109 Å/cycle obtained by the QCM measurements and the *ex situ* growth rate of 37.6 Å/cycle derived by the XRR measurements during the linear growth region.

The differences between the *in situ* and the *ex situ* growth rates may result from changes that occur upon exposure of ABC films to ambient. For example, diffusion of TMA out of the film may occur upon exposure to air. This TMA out diffusion could lead to a mass loss from the *in situ* QCM measurements to the *ex situ* XRR measurement. This mass loss could explain the lower growth rate for the ABC films exposed to air. Another explanation for the different growth rates could be a changing density for the ABC film upon air exposure. For example, reorganization of the ABC film structure, perhaps resulting from the removal of TMA, could lead to the expansion of the film. A smaller film density after air exposure would lead to larger effective film thicknesses from the measured mass gains.

The stability of the ABC films was also investigated using XRR analysis. Progressive XRR scans of the same ABC film grown at 90 °C were recorded versus time after removing the sample from the reactor. A slight increase was observed in the XRR oscillation period. The largest change of the ABC film occurred in the first ~50−70 h, with a nearly constant thickness reached after ~300 h. After aging in air, the ABC film thickness decreased by 5.8%. In comparison, previous stability analysis of alucone MLD films grown with TMA and EG observed thickness decreases of ~20%.[12]

F. Measurement and Modeling of TMA Diffusion. The diffusion of TMA into and out of the ABC film was measured experimentally and then fit using a numerical model. Figure 8 shows the mass gain measured for a 200 s TMA dose followed by 800 s purge at 110 °C. Immediately prior to the results shown in Figure 8, 30 MLD cycles of ABC were grown at 110 °C onto an Al_2O_3 ALD surface ending with a MA exposure. This ABC film had an estimated thickness of 400 Å. The 200 s TMA dose led to a mass gain of 1776 ng/cm^2. A slow mass loss then occurred during the TMA purge period. The result was a net mass gain of 1550 ng/cm^2 after the 800 s purge. These large mass gains at 110 °C are attributed to both TMA reaction with MA surface species and TMA absorption by the ABC film.

To support the TMA diffusion argument, the mass gain and mass loss were fitted using numerical diffusion simulations in Figure 8. For the TMA diffusion into the ABC film, the fitted diffusion constant was $D_1 = 2 \times 10^{-16}$ m^2/s. The TMA concentration profile at the starting point of the TMA diffusion out process was then scaled by a factor $f = 0.127$ to account for the fact that only 226 ng/cm^2 out of 1776 ng/cm^2 of TMA are available for diffusion. The fitted diffusivity for the TMA diffusion out process was $D_2 = 1.4 \times 10^{-16}$ m^2/s. The magnitude of the diffusion coefficients into and out of the ABC film, D_1 and D_2, are very comparable. The slightly lower magnitude for D_2 may be caused by the modification of the ABC film by the TMA reaction and absorption.

G. Comparison with Previous FTIR Studies. The importance of TMA diffusion revealed by the QCM studies in the current study was not obvious in the previous FTIR studies of the ABC MLD surface chemistry.[17] The previous FTIR analysis did not observe the effects of TMA diffusion because the FTIR studies were conducted primarily at higher temperatures of 150 °C.[17] At this higher temperature, there is less TMA diffusion into the ABC film, the TMA residence time in the ABC film is shorter, and the

(31) Kerle, T.; Lin, Z. Q.; Kim, H. C.; Russell, T. P. *Macromolecules* **2001**, *34*, 3484.
(32) Jones, R. A. L. *Curr. Opin. Colloid Interface Sci.* **1999**, *4*, 153.

ABC growth rates are much lower. Figure 7 shows that the ABC film growth does not enter the large growth region at 150 °C even after 50 MLD cycles.

The FTIR spectra were also recorded during the initial MLD cycles of ABC film growth. The FTIR studies were performed on nanoparticles to obtain higher surface areas to enhance the surface sensitivity of the transmission FTIR experiments. The surface area is reduced as the MLD film fills the volume between the nanoparticles. Consequently, most of the FTIR spectra were recorded during the first 5−15 MLD cycles. As shown in Figures 1 and 7, the ABC film growth does not enter the large growth region until >20 MLD cycles. The higher temperatures and lower number of MLD cycles used in the FTIR experiments prevented the FTIR studies from determining the effects of TMA diffusion on ABC film growth.

The FTIR studies also observed that the absorbance for the vibrational modes of the ABC film grew linearly with the number of MLD cycles during the first 7 MLD cycles.[17] In this initial growth regime, the number of active surface species is constant. The constant growth indicates that an average of 1.5 S−COOH* species react with each TMA precursor in eq 1.[23] There is not a doubling of the number of reactive sites where each S−COOH* would become 2 $AlCH_3$* species. In addition, the FTIR studies observed that some $AlCH_3$* species are left behind as unreacted $AlCH_3$* species in the growing film.[17] These $AlCH_3$* species can react with H_2O in air and add additional absorbance for O−H stretching vibrations in the film.[17]

IV. Conclusions

Hybrid organic−inorganic MLD films were grown using a three-step ABC sequence of trimethylaluminum (TMA), ethanolamine (EA), and maleic anhydride (MA). Film growth during MLD was studied using *in situ* quartz crystal microbalance (QCM) studies in a viscous flow reactor. The ABC growth on Al_2O_3 ALD surfaces displayed distinct growth regions. Initially, a low mass gain per cycle is observed while the ABC film begins to grow on the Al_2O_3 ALD substrate. The mass gain per cycle increased with increasing ABC film thickness. The mass gains per cycle measured by the QCM studies then reached a large constant steady state value of 1854−4220 ng/(cm^2 cycle) under a variety of reaction conditions at 90 °C.

The QCM mass profiles indicated that the large growth rates were caused by TMA diffusion into the ABC film. Although some TMA also diffuses out of the ABC film, the remaining TMA is available to react with EA in a chemical vapor deposition (CVD) reaction that adds to the MLD surface reaction. Corroboration of the importance of TMA diffusion was provided by the dependence of the ABC growth rate on both the TMA dose and TMA purge times. Multidose experiments conducted in the initial nucleation region at 130 °C observed self-limiting behavior for thin ABC films. In contrast, the multidose experiments revealed strong evidence for TMA diffusion and non-self-limiting behavior in the steady state growth region on thick ABC films.

Although the ABC films result in part from a CVD reaction between TMA and EA, X-ray reflectivity (XRR) measurements revealed that the ABC films were extremely smooth. XRR studies also observed that the ABC films decreased slightly in thickness by ~5% in the first few days after growth before displaying very stable behavior. Numerical modeling assuming Fickian diffusion for TMA diffusing into and out of the ABC film was able to fit the QCM mass profiles. These studies illustrate that precursor diffusion into the MLD film makes an important contribution to the MLD film growth mechanism.

Acknowledgment. This work was funded by the National Science Foundation under Grant CHE-0715552. D.S. also acknowledges support from DARPA NEMS (SPAWAR Contract No. N66001-07-1-2033, DARPA Award #HR0011-06-1-0048). Some of the equipment used in this research was provided by the Air Force Office of Scientific Research. The authors acknowledge Zachary Gibbs for helpful discussions on the diffusion modeling.